Starting energy dependence of elastic scattering observables in a full-folding model

H. F. Arellano and W. G. Love
Department of Physics and Astronomy, University of Georgia, Athens, Georgia 30602

F. A. Brieva
Departamento de Física, Facultad de Ciencias Físicas y Matemáticas, Universidad de Chile, Casilla 487-3, Santiago, Chile

(Received 9 January 1991)

Full-folding model calculations of proton elastic scattering at intermediate energy made using the free off-shell *NNt* matrix and including the variation of the energy in the *NN* center of mass as prescribed by the full-folding model are compared with similar calculations using *t* matrices evaluated at a fixed energy. The fixed energy is chosen on the basis of the incident beam energy ignoring the Fermi momentum of the struck target nucleon. Near 200 MeV, the energy prescription for the *NNt* matrix is found to be responsible for much of the difference between recently reported full-folding calculations as well as for the differences between full-folding calculations and conventional $t\rho$ approximations to them. The sensitivity of the scattering observables to the starting energy suggests that at lower intermediate energies, explicit medium corrections should be included in applications of the full-folding model.

I. INTRODUCTION

The problem of understanding elastic scattering in terms of the nucleon optical potential continues to receive considerable attention as one of the critical problems of nuclear physics. Following the introduction of medium corrections[1] and relativistic degrees of freedom[2] within primarily local models, important off-energy-shell effects have recently been reported in nonrelativistic full-folding calculations of the nucleon optical potential.[3–5] Within the full-folding framework it is found that an explicit and accurate treatment of the off-shell behavior of the nucleon-nucleon (NN) effective interaction yields important corrections to the traditional nonrelativistic local $t\rho$ approach.

Different groups[3–5] have followed alternative approaches in order to assess the importance of the off-shell effects in calculations of nucleon-nucleus (NA) couplings for intermediate-energy nucleon scattering. These approaches differ mainly in their choices of the starting energy available for the interacting nucleon pair. Thus, results of full-folding calculations[4,5] in which the available energy in the *NN* center of mass (propagating energy) is held *fixed* differ only slightly from those obtained using an optimally factorized version of the off-shell $t\rho$ approximation. This has been demonstrated in Ref. 4 using the full-Bonn[6] *NN* potential and in Ref. 5 using the Paris[7] potential. In contrast to these findings are the results of Ref. 3 in which the *variation* of the *NN* c.m. energy prescribed by the full-folding model was treated explicitly. In this latter work,[3] which uses the Paris potential, differences between the full-folding results and those obtained using the optimally factorized version of the off-shell $t\rho$ approximation are substantial.

In light of the newness and complexity of full-folding-type calculations, it is important to understand the differences which arise between apparently similar calculations. Accordingly, in this work we examine in some detail the energies and momenta characteristic of the full-folding model when the *NN* effective interaction is represented by the free *t* matrix. In particular, we study the sensitivity of the calculated scattering observables to the treatment of the *NN* propagating energy which is required for evaluating the *NN t* matrix. Somewhat similar studies, with an emphasis on pion-nucleus scattering, have been made in Ref. 8. There the authors find a strong sensitivity to the choice of the energy in the propagator when a resonance region in the projectile-nucleon system is sampled. In the case of proton-nucleus scattering, we find that the different treatments of the propagating energy account for most of the differences observed in recent results obtained from a nonrelativistic full-folding model.

In Sec. II the relationship between the kinematics and different choices for the starting energy is outlined and discussed within the full-folding framework. In Sec. III calculated scattering observables are compared using the three different choices for the starting energy described in Sec. II. In Sec. IV the sensitivity of the full-folding results to the *NN* propagating energy is made relatively transparent by studying a Fermi-averaged *NN t* matrix which is derived using a simple model of the mixed density of the target ground state. Section V contains our summary and conclusions.

II. KINEMATICS AND STARTING ENERGIES

Ignoring recoil effects and medium corrections, and assuming a single-particle description for the target ground state, the nonrelativistic full-folding optical potential can be expressed as[3]

$$U(\mathbf{k}',\mathbf{k};E)=\sum_{\alpha}\int d\mathbf{P}\ \varphi_{\alpha}^{\dagger}(\mathbf{p}')\langle\kappa'|\hat{t}(z_{\alpha})|\kappa\rangle_{\mathcal{A}}\varphi_{\alpha}(\mathbf{p})\ , \quad (1)$$

where φ_α denotes a single-particle state with energy ε_α and the summation over α is restricted to occupied states. The momenta $\mathbf{p}$ and $\mathbf{p}'$ correspond to those of the struck target nucleon before and after its collision with the projectile, respectively, and are given by $\mathbf{p}'=\mathbf{P}+\frac{1}{2}\mathbf{q}$, $\mathbf{p}=\mathbf{P}-\frac{1}{2}\mathbf{q}$, with $\mathbf{q}$ given by $\mathbf{q}=\mathbf{k}-\mathbf{k}'$. The integration variable $\mathbf{P}$ represents the mean momentum of the struck nucleon before and after its collision with the projectile $[\mathbf{P}=\frac{1}{2}(\mathbf{p}+\mathbf{p}')]$ or, alternatively, the nuclear convection current times the nucleon mass. The *NN* effective interaction is represented by the free t matrix $\hat{t}(z)$ which satisfies the Lippmann-Schwinger equation

$$\hat{t}(z)=v+v\frac{1}{z-K+i\eta}\hat{t}(z)\ , \quad (2)$$

with v the *NN* bare potential and K the kinetic-energy operator for the relative motion. The t matrix is evaluated at the incoming (outgoing) relative momentum κ (κ') and a propagating energy in the *NN* c.m. system z_α which are given by

$$\kappa'=\tfrac{1}{2}(\mathbf{K}-\mathbf{P}-\mathbf{q})\quad \kappa=\tfrac{1}{2}(\mathbf{K}-\mathbf{P}+\mathbf{q})$$
$$z_\alpha=\omega_\alpha-(\mathbf{P}+\mathbf{K})^2/2M\ , \quad (3)$$

with $\mathbf{K}=\frac{1}{2}(\mathbf{k}+\mathbf{k}')$ the mean momentum of the projectile or its convection current times its mass. Here ω_α (the two-nucleon starting energy) is given by $E+\varepsilon_\alpha$, with E the kinetic energy of the projectile in the *NA* c.m. In Eqs. (3) M represents the mass of the interacting pair whose total momentum in the *NA* c.m. is $\mathbf{P}+\mathbf{K}$. The above prescription for the *NN* propagating energy (z_α) is obtained by reducing the many-body propagator in the Watson[9] and Kerman, McManus, and Thaler[10] theories for *NA* scattering to a two-body propagator assuming a shell model for the target nucleons in the nucleus. Modifications of the propagator due to distortion in intermediate states are neglected and only those intermediate states in the continuum are taken into account.[3] These approximations lead to the use of the free *NN* t matrix as the *NN* effective interaction. Although medium modifications arising from the effect of the nuclear field and from the restrictions imposed by the Pauli principle on allowable intermediate states (particularly those near the Fermi surface) should be included, calculations of optical potentials which include these modifications consistently within the full-folding framework are presently unavailable.

In order to better understand the kinematics implicit in the momentum and energy variables needed in the *NN* t matrix for calculating the optical potential [Eq. (3)], it is helpful to consider the total energies associated with the initial (e) and final (e') states of the colliding particles. In the absence of self-energy corrections these are

$$e=\frac{\mathbf{k}^2}{2m}+\frac{(\mathbf{P}-\frac{1}{2}\mathbf{q})^2}{2m}=\frac{1}{2\mu}\kappa^2+\frac{1}{2M}(\mathbf{K}+\mathbf{P})^2\ , \quad (4a)$$

$$e'=\frac{\mathbf{k}'^2}{2m}+\frac{(\mathbf{P}+\frac{1}{2}\mathbf{q})^2}{2m}=\frac{1}{2\mu}\kappa'^2+\frac{1}{2M}(\mathbf{K}+\mathbf{P})^2\ , \quad (4b)$$

where μ is the reduced mass of the *NN* pair. The quantities $\kappa^2/2\mu$ and $(\mathbf{P}+\mathbf{K})^2/2M$ are the relative and c.m. energies of the colliding pair. These energies e and e' can be compared to the total (starting) energy of the propagating *NN* pair $E+\langle\varepsilon_{p,n}\rangle$, where the single-particle energy ε_α has been replaced by the proton (neutron) single-particle energy average $\langle\varepsilon_{p(n)}\rangle$ obtained from the shell model used to describe the target nucleus. Henceforth the labels p and n appearing in z and ε shall be omitted. Since, in the present approach, the c.m. energy is conserved, this approach provides a direct measurement of how far off shell the t matrix needs to be evaluated.

A simple analysis of the energies $(e',e;\omega)$ can be made by considering the kinematics associated with off-shell t-matrix contributions to the on-shell matrix elements of the optical potential. In this case the momenta of the projectile $\mathbf{k}$ and $\mathbf{k}'$ are constrained by $|\mathbf{k}'|=|\mathbf{k}|$ and $E=k^2/2m$. Furthermore, we let the orientation of $\mathbf{P}$ vary in the plane defined by $\mathbf{k}$ and $\mathbf{k}'$ as shown in Fig. 1, where β denotes the angle between $\mathbf{P}$ and $\mathbf{K}$. In order to estimate the initial- and final-state energies relative to the total energy ω, $\omega=E+\langle\varepsilon\rangle$, we consider the differences

$$e'-\omega=\frac{1}{2m}(\mathbf{P}+\tfrac{1}{2}\mathbf{q})^2-\langle\varepsilon\rangle=\frac{1}{2m}p'^2-\langle\varepsilon\rangle\geq 0\ , \quad (5a)$$

$$e-\omega=\frac{1}{2m}(\mathbf{P}-\tfrac{1}{2}\mathbf{q})^2-\langle\varepsilon\rangle=\frac{1}{2m}p^2-\langle\varepsilon\rangle\geq 0\ , \quad (5b)$$

$$e'-e=\frac{1}{m}\mathbf{q}\cdot\mathbf{P}=\frac{1}{m}qP\sin\beta\ . \quad (5c)$$

From these relations the occurrence of off-shell (*NN*) contributions to the on-shell (*NA*) matrix elements of the optical potential becomes evident as long as the motion of the target nucleons and their binding are taken into account. Considering that typical values of p and p' are of the order of 1 fm^{-1} and the average binding energy $\langle\varepsilon\rangle\approx-25$ MeV, the difference $e(e')-\omega$ is roughly 45 MeV. This difference does not depend on the energy of the beam so that its importance relative to the beam energy decreases as the latter increases.

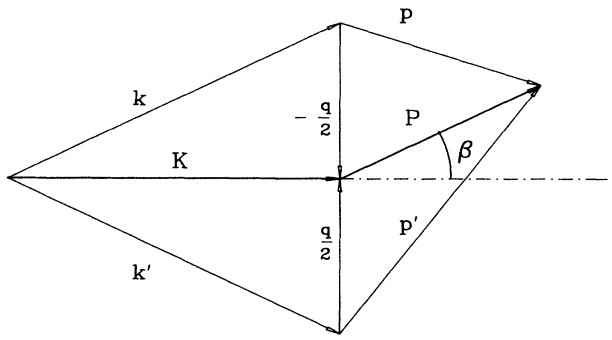

FIG. 1. Kinematics associated with on-shell matrix elements of the optical potential.

It is also interesting to follow, in the on-shell situation discussed above, the behavior of the energies $(e',e;\omega)$ as functions of β, the angle between the projectile and struck nucleon currents (Fig. 1). As the angle β varies we can compare the magnitudes of the total final, initial, and starting energies and illustrate the occurrence of off-shell processes at the NN level. In Fig. 2 we show a polar plot of the energies e',e,ω, and the NN c.m. energy $(\mathbf{K}+\mathbf{P})^2/2M$ which we label $E_{\text{c.m.}}$. The solid curves labeled with e and e' represent the NN total energies before and after their collision, respectively. The dashed and dash-dotted curves represent the starting energies when given by $\omega=k^2/2m$ (labeled ω_0) and $\omega=k^2/2m+\langle\varepsilon\rangle$ (labeled ω_ε),respectively. The curves shown in Fig. 2 correspond to a beam energy of 200 MeV. We have chosen $q=1$ fm^{-1} based on the fact that most of the features peculiar to full-folding calculations occur for $q\lesssim 2$ fm^{-1}, and $P=0.8$ fm^{-1} since the target mixed density times P^2 peaks around this value of $\mathbf{P}$.[11] The average binding energy, $\langle\varepsilon\rangle$ is taken to be -25 MeV. We observe two distinct features at $\beta=0$ and $\beta=\pm 90°$. In the first case we note that the initial and final energies are equal, as given by Eq. (5c), and differ by $(P^2+\frac{1}{4}q^2)/2m-\langle\varepsilon\rangle$ from the starting energy. This difference represents the amount by which the NN collision is off shell and is determined by the values of P and $\langle\varepsilon\rangle$, which are characteristic of each target, and by the relevant momentum transfers q. In the case of $\beta=90°$ the difference $e'-e$ is qP/m. For $q\sim 2$ fm^{-1} and assuming $P\sim 1$ fm^{-1} this difference amounts to ~ 80 MeV and decreases linearly with q. As we increase the energy of the beam the differences among e,e', and ω become negligible relative to E. Indeed, in the high-energy limit the curves for e,e' and ω become concentric circles of radius $\sim E$ as P,q, and $\langle\varepsilon\rangle$ become less important. At low energies, however, the situation is quite different. In this case the differences between the energies e,e', and ω can be comparable to the energy of the beam. A reliable assessment of the importance of the kinematics represented in Fig. 2 for the purpose of describing NA scattering can only be made through actual calculations of the full-folding optical potential.

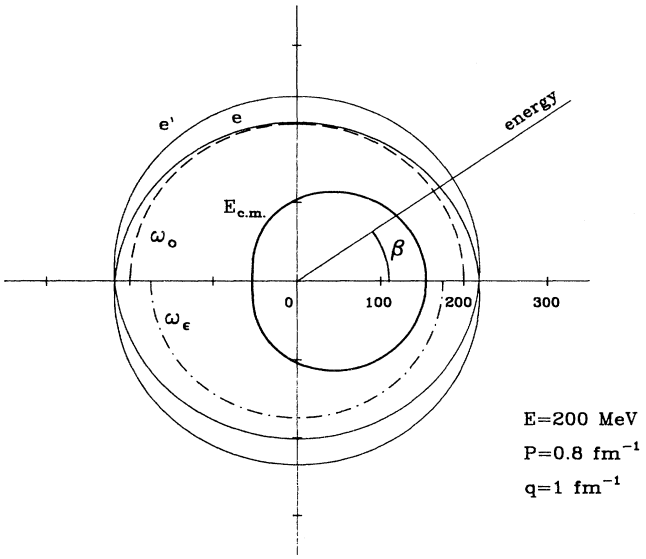

FIG. 2. Total initial (e) and final (e') energies of the nucleon pair as functions of β. The dashed and dot-dashed circles represent the starting energy when binding is neglected (ω_0) and included (ω_ε), respectively. The dark solid curve represents the energy carried by the NN c.m.

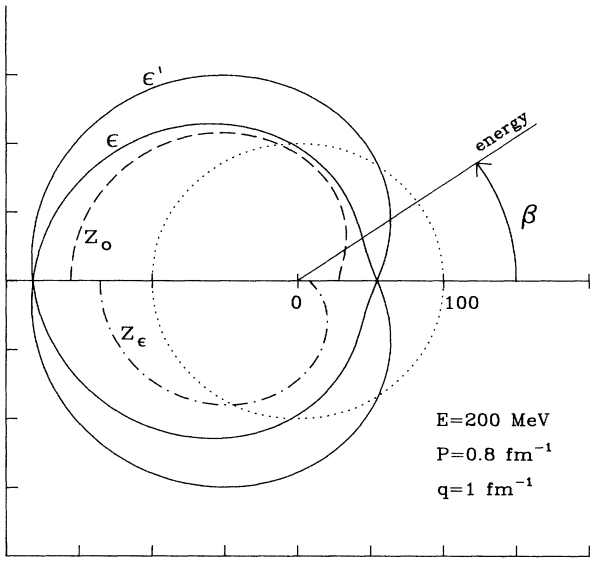

FIG. 3. Relative initial (ϵ) and final (ϵ') energies of the nucleon pair as functions of β. The dashed and dot-dashed circles represent the propagating energies in the NN c.m. (z) when binding is neglected (z_0) and included (z_ε), respectively. The dotted curve represents a fixed energy equal to $\frac{1}{2}E$.

One important aspect of Fig. 2 is the energy $E_{\text{c.m.}}$ carried by the NN c.m. This energy varies as the angle β changes, being a maximum (minimum) when the projectile and struck nucleon currents are parallel (antiparallel). As a result, for a given β, the energy available in the c.m. of the NN pair varies as the radial difference between $E_{\text{c.m.}}$ and (e,e',ω). For further clarity, and to have some measure of the quantities which actually enter in evaluating the NN t matrix in Eq. (1), we plot in Fig. 3 the energies in the NN c.m. system $\epsilon'=e'-E_{\text{c.m.}}$, $\epsilon=e-E_{\text{c.m.}}$, and $z=\omega-E_{\text{c.m.}}$ as functions of β. The circle (dotted curve) in Fig. 3 represents a fixed energy equal to $\frac{1}{2}E$; its significance will be discussed later. We observe in Fig. 3 an overall tendency of lower-energy NN collisions when the projectile and struck nucleon currents are parallel. When these currents are in opposite directions the situation is reversed leading to higher-energy collisions in the NN c.m. We stress that the situation depicted in Fig. 3 is more complicated when considering arbitrary (off-shell) matrix elements of the optical potential.

III. RESULTS

One of the main objectives of this work is focused on the role of the NN propagating energy in the full-folding model for which we consider three alternative treatments of z_α [Eq. (3)]. The first is essentially that indicated in Eq. (1) with the exception that each ε_α is approximated by $\langle\varepsilon\rangle$ which should be adequate at high and intermedi-

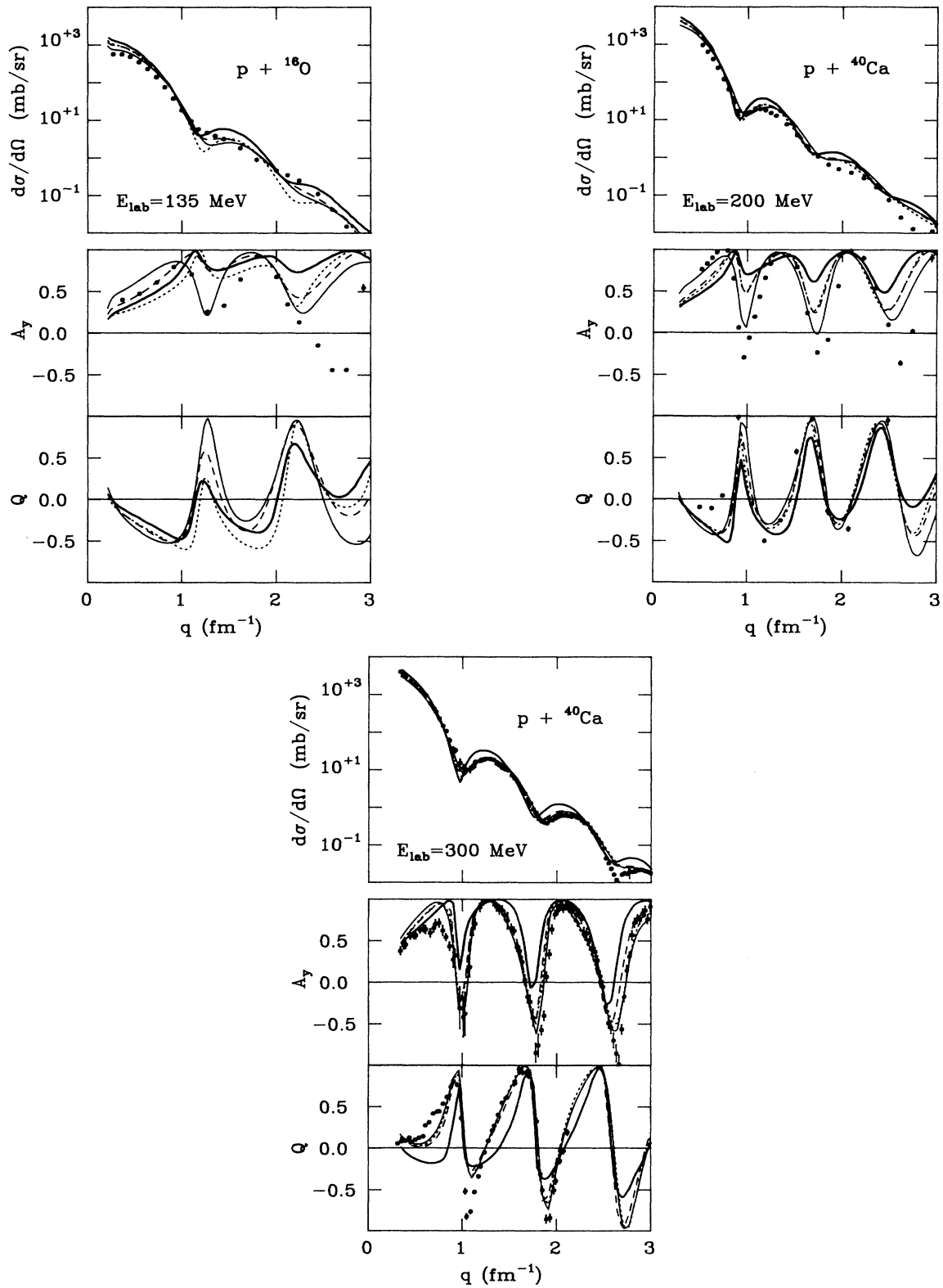

FIG. 4. Calculated and measured scattering observables for $p+{}^{16}\mathrm{O}$ and $p+{}^{40}\mathrm{Ca}$ elastic scattering. The *light* solid and dashed curves correspond to full-folding calculations using variable energy including and neglecting binding, respectively; the dotted curves were obtained using fixed energy and neglecting binding. The *dark* solid curves correspond to calculations using the on-shell $t\rho$ approximation to the optical potential. The $p+{}^{16}\mathrm{O}$ scattering data at 135 MeV were taken from Ref. 12. The data for $p+{}^{40}\mathrm{Ca}$ at 200 and 300 MeV were taken from Refs. 13 and 14, respectively. The Q data shown at 300 MeV correspond to measurements made at 320 MeV taken from Ref. 15.

ate incident energies. The second approach is the same as the first except that $\langle \varepsilon \rangle$ is set equal to zero. The third approach involves approximating z by a fixed value equal to roughly one-half of the beam energy. The latter treatment is based on the assumption of a relatively weak dependence of the NN t matrix on the available energy, z. Thus, one neglects variations in the propagating energy due to variations of $\mathbf{P}$ and $\mathbf{K}$ by setting $\mathbf{P}$ equal to zero and $\mathbf{K}$ to a fixed value corresponding to forward scattering for the on-shell contribution ($\mathbf{K}=\mathbf{k}=\mathbf{k}', E=k^2/2m$). These considerations yield $z=E/2+\langle \varepsilon \rangle$ which, apart from the binding energy $\langle \varepsilon \rangle$, has been the energy prescription adopted in some of the recent full-folding types of calculations for intermediate-energy proton-nucleus scattering.[4,5] In the context of the discussion of Fig. 3, the fixed-energy prescription yields $z=100$ MeV $+\langle \varepsilon \rangle$ independent of β while ε and ε' retain their dependence on $\mathbf{P}$. In such a case the fixed-energy prescription requires matrix elements farther off shell than those prescribed by the full-folding procedure. This effect can also be visualized in the context of Fig. 2. Indeed, the fixed energy prescription implies a starting energy given by $\omega=\frac{1}{2}E+(\mathbf{K}+\mathbf{P})^2/2M+\langle \varepsilon \rangle$.

In order to study the dependence of full-folding optical potentials on the choice of the propagating energy z we have performed calculations for proton elastic scattering from ^{16}O and ^{40}Ca between 135 and 300 MeV, an energy range where the full-folding model has been shown to provide a reasonable description of the scattering observables. For calculating the optical potential the single-particle states were generated in a Woods-Saxon well as described in Ref. 3 and the Paris NN potential was used to generate the fully off-shell NN t matrix. Full-folding results shown here were made using sets of t matrices calculated at six values of the NN c.m. energy distributed nearly uniformly between 1 MeV and $\sim E_{\rm lab}$. These calculations were made as described in Ref. 3 and used $\langle \varepsilon_p \rangle=-23.8$ MeV and $\langle \varepsilon_n \rangle=-27.3$ MeV in the case of ^{16}O and $\langle \varepsilon_p \rangle=-24.0$ MeV and $\langle \varepsilon_n \rangle=-31.4$ MeV for ^{40}Ca. The elastic scattering observables for proton scattering presented here were obtained using momentum-space procedures; results obtained using coordinate-space procedures are nearly indistinguishable[3] from these, thus showing no ambiguity in the treatment of the Coulomb potential.

The primary results of this work are shown in Fig. 4 where full-folding calculations using different treatments of the NN propagating energy are compared to the traditional on-shell $t\rho$ approximation for $p+^{16}$O and $p+^{40}$Ca elastic scattering at 135, 200, and 300 MeV beam energy. The measured observables are also shown for reference. The *dark* solid curves represent results using the on-shell $t\rho$ approximation to the optical potential. The *light* solid and dashed curves correspond to full-folding calculations where the average binding energy in the starting energy is included and excluded, respectively; the dotted curves represent full-folding calculations in which the propagating energy has been fixed at one-half the beam energy in the NA c.m. The latter case is equivalent to the full-folding calculations presented in Refs. 4 and 5. As noted in Refs. 3–5, there are significant differences at each energy between the full-folding results and those using the on-shell $t\rho$ approximation. In addition, there are also noticeable differences among full-folding calculations at energies below $\sim$200 MeV. We note in this case that the inclusion of the binding energy of the struck nucleons in the starting energy *and* the explicit treatment of the variation of the NN propagating energy [$z\sim E+\langle \varepsilon \rangle -(\mathbf{P}+\mathbf{K})^2/2M$] lead to a considerable improvement in the description of the spin observables. In the case of $p+^{16}$O scattering at 135 MeV the sensitivity of the scattering observables to different treatments of the NN propagating energy is more noticeable. In the case of $p+^{40}$Ca scattering at energies above $\sim$300 MeV this sensitivity diminishes substantially. At 200 MeV and below we observe a clear sensitivity to the details of the treatment of the NN propagating energy. Although the full-folding calculations which use Eqs. (3) to sample the NN effective interaction off shell provide a superior description of the data within the energy range considered here, it is necessary to make reliable estimates of the importance of medium effects in a full-folding framework, particularly in light of the sensitivity of the results to binding energy corrections.

The results shown in Fig. 4 and discussed above are consistent with those presented in Refs. 4 and 5. In Refs. 4 and 5 the authors compare scattering observables obtained from full-folding optical potentials using the fixed-energy prescription for the NNt-matrix and its associated off-shell $t\rho$ approximation and find very little difference between the two approaches. We have also compared elastic scattering observables in these two approximations and they agree closely with those presented by Crespo, Johnson, and Tostevin[5] where the Paris NN potential is used. Therefore, the quantitative differences between the full-folding calculations presented in Refs. 3 and 5 are due to the differences in the treatment of the NN propagating energy.

IV. A FERMI-AVERAGED NN t MATRIX

In order to make some of the features introduced in full-folding calculations of the optical potential more transparent and to compare them with those in alternative approximations, we consider a recently proposed approximation to the full-folding optical potential.[11] As shown in Ref. 11 most of the characteristic features of the full-folding optical potential are well described by using a Slater-type approximation for the target mixed density. In this approximation it is necessary to neglect the *variation* of the single-particle energies by considering the average value $\langle \varepsilon \rangle$ as was done above. With this assumption one can rewrite the optical potential as

$$U(\mathbf{k}'\mathbf{k};E)=\int d\mathbf{P}\,\rho(\mathbf{p}',\mathbf{p})\langle \boldsymbol{\kappa}'|\hat{t}(z)|\boldsymbol{\kappa}\rangle \ , \tag{6}$$

where ρ denotes the target mixed density (neutrons or protons),

$$\rho(\mathbf{p}',\mathbf{p})=\sum_{\alpha}\varphi_{\alpha}^{\dagger}(\mathbf{p}')\varphi_{\alpha}(\mathbf{p}) \ . \tag{7}$$

Using a Slater form for the nonlocality function of the mixed density, $\rho(\mathbf{p}',\mathbf{p})$ can be expressed in terms of the moduli of $\mathbf{P}$ and $\mathbf{q}$ of Eq. (2) as [11]

$$\rho(\mathbf{p}',\mathbf{p}) \simeq \rho(P;q) = \frac{1}{(2\pi)^3}\left[4\pi\int_0^\infty R^2 dR \frac{\rho(R)}{\hat{\rho}(R)} j_0(qR)\Theta(\hat{k}_R - P)\right], \tag{8}$$

where $\hat{k}_R$ is a local momentum function obtained from the Campi-Bouyssy or Slater approximation[11] which depends on R and defines the function $\hat{\rho}$ by

$$\hat{\rho}(R) = \frac{1}{3\pi^2}\hat{k}_R^3 . \tag{9}$$

With the use of the above form for the mixed density, Eq. (6) for the optical potential may be rewritten as

$$U(\mathbf{k}',\mathbf{k};E) = 4\pi\int_0^\infty R^2 dR\, \rho(R) j_0(qR)\hat{t}_{\rm av}(\mathbf{k}',\mathbf{k};\hat{k}_R;E) , \tag{10}$$

where one has introduced an average t matrix

$$\hat{t}_{\rm av}(\mathbf{k}',\mathbf{k};\hat{k}_R;E) = \frac{1}{\frac{4}{3}\pi\hat{k}_R^3}\int d\mathbf{P}\langle\kappa'|\hat{t}(z)|\kappa\rangle\Theta(\hat{k}_R - P) . \tag{11}$$

Apart from the explicit dependence of $\hat{t}_{\rm av}$ on the coordinates $\mathbf{k}',\mathbf{k}$ and $\hat{k}_R$, Eq. (10) for the optical potential displays a structure similar to the traditional (and local) $t\rho$ approximation. However, we note that the average t matrix incorporates explicitly the off-shell behavior of the NN effective interaction as required by the full-folding model and given by Eqs. (3). This feature is particularly appealing since a study of the behavior of $\hat{t}_{\rm av}$ allows one to gauge the sensitivity of full-folding-like calculations to different approximations made in evaluating the NN effective interaction. In particular, and for the purpose of the present discussion, we examine the behavior of $\hat{t}_{\rm av}$ as a function of q at on-shell values of $\mathbf{k}$ and $\mathbf{k}'$ in the NA c.m. for different treatments of the propagating energy.

In Fig. 5 we show the central isoscalar ($\Delta T=0$) component of $\hat{t}_{\rm av}$ as a function of q for different values of the beam energy E. The curve patterns used here follow the same convention as those used in Fig. 4: the dark solid

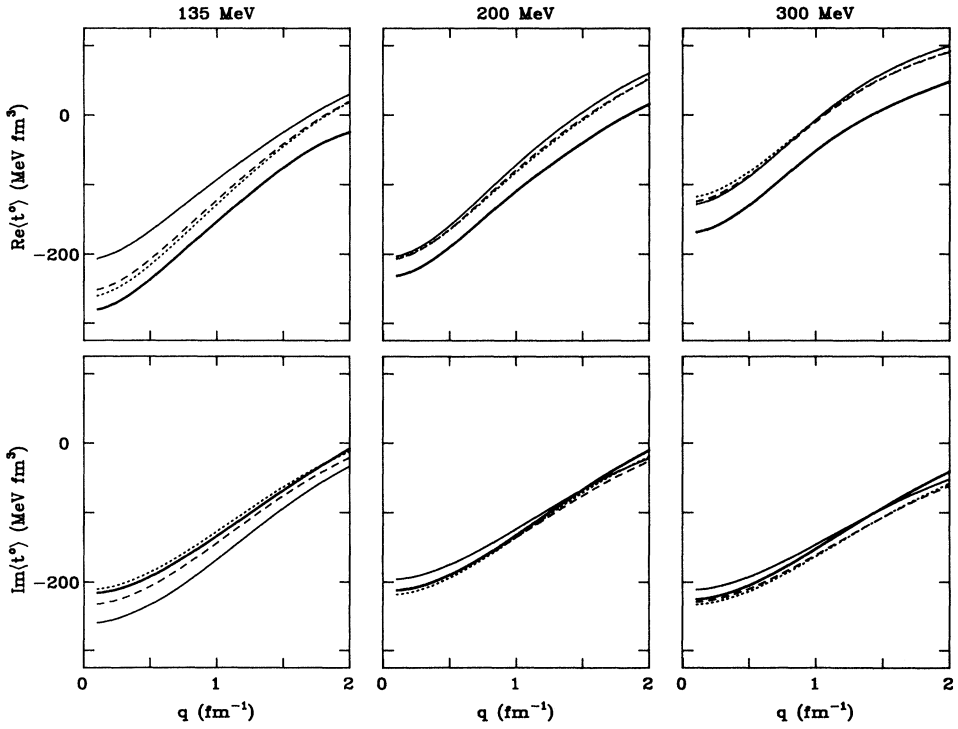

FIG. 5. The isoscalar ($\Delta T=0$) off-shell average free t matrix as a function of q. Light-solid, dashed and dotted curves include off-shell effects as defined in Eq. (11). The dark solid curves correspond to the on-shell t matrix using the "optimum energy prescription" (Ref. 3).

curves represent t on shell as a function of q with z given by the "optimum energy approximation";[3] the lighter solid curves represent results using $z=E+\langle\varepsilon\rangle-(\mathbf{P}+\mathbf{K})^2/2M$, with $\langle\varepsilon\rangle=-25$ MeV; the dashed curves correspond to $z=E-(\mathbf{P}+\mathbf{K})^2/2M$; the dotted curves correspond to $z=\frac{1}{2}E$. The amplitudes $\hat{t}_{\rm av}$ are calculated using $\hat{k}_R=1$ fm,$^{-1}$ based on the expectation that the dominant contributions to the optical potential should occur where the distribution $R^2\rho(R)$ is localized [see Eq. (10)]. In the case of ^{40}Ca, this consideration leads to values of R in the range $R\sim 2$–4 fm, for which $\hat{k}_R$ varies between[11] ~ 1 and 1.3 fm.$^{-1}$

In Fig. 5 we observe that, at each of the energies considered, the on-shell t matrix is more attractive than each of the effective interactions in which the full-folding effects are incorporated through the average procedure. In the 135-Mev case, the differences among the different treatments used for z are especially noticeable. At this energy we note that the variable-energy prescription *with* the binding-energy term in the starting energy makes the NN interaction less attractive than in the case of fixed energy or variable energy without binding. At 200 and 300 MeV, these differences are less pronounced. On the other hand, at each energy the imaginary part of the NN effective interaction shows sensitivity to the inclusion/exclusion of the binding energy in the starting energy. With the exception of the 135-MeV case, the imaginary part of $\hat{t}_{\rm av}$ obtained when including the binding energy in the starting energy is less absorptive than observed in each of the other approaches considered. Furthermore, we note at these energies that the $\mathrm{Im}\langle\hat{t}_{\rm av}\rangle$ based on full-folding procedures are "flatter," and therefore of shorter range, than the on-shell NN interactions. This property of $\hat{t}_{\rm av}$ corresponds to an effective local NA potential with a shorter range than is characteristic of the on-shell $t\rho$ model and accounts for the shifts in the diffraction minima in the cross sections to larger angles relative to those in the on-shell $t\rho$ model. Overall, in Fig. 5 we note that the fixed-energy prescription in the full-folding approach yields a $\hat{t}_{\rm av}$ which is very similar to that obtained when the variation of the energy is treated explicitly and the binding energy of the struck nucleon is ignored. A study of the spin-orbit contributions similar to those discussed here shows significantly less sensitivity to the different treatments of the NN propagating energy.

V. SUMMARY AND CONCLUSIONS

We have studied the sensitivity of the full-folding optical potential for intermediate-energy elastic scattering to different treatments of the NN propagating energy. In particular, we have focused on the role of the variation of the NN propagating energy due to the motion of the struck-target nucleons and on the importance of the average binding energy in the starting energy. At energies above ~ 300 MeV the full-folding calculation results are relatively insensitive to different treatments of the NN propagating energy. As the beam energy is lowered the full-folding results become increasingly sensitive to the treatment of the NN energy. In particular, we note that the inclusion of the binding energy of the struck nucleon in the starting energy, along with an accurate treatment of the motion of the struck nucleon, are the main features which provide the closest agreement of full-folding calculations with the data within a scheme in which the free t matrix is used to represent the NN effective interaction, particularly in applications at lower energies. Given the sensitivity of full-folding calculations in applications at these lower energies, where the strongly energy-dependent S-wave part of the t matrix is sampled by the large-momentum components of the bound-state wave functions, we expect that the inclusion of explicit medium effects beyond those included by averaging over the Fermi motion are needed in order to more reliably assess the adequacy of the nonrelativistic theory for NA scattering.

In this work we have introduced an average t matrix which incorporates explicitly the off-shell behavior of the NN effective interaction as required by the full-folding model. The interesting feature of this average t matrix is that it provides a simple scheme for gauging the sensitivity to different approximations used in evaluating the NN effective interaction in full-folding-like calculations.

ACKNOWLEDGMENTS

This work was supported in part by NSF Grant No. PHY-8903856. F.A.B. acknowledges partial support from the Fondo Nacional de Desarrollo Científico y Tecnológico, Chile, Grant No. 1239-90. We also appreciate a grant for computing time provided by the University of Georgia.

[1]L. Rikus and H. V. von Geramb, Nucl. Phys. **A426**, 496 (1984); H. V. von Geramb, in *The Interaction Between Medium Energy Nucleons in Nuclei,* edited by H. O. Meyer (AIP, New York, 1983).

[2]N. Ottenstein, S. J. Wallace, and J. A. Tjon, Phys. Rev. C **38**, 2272 (1988); D. P. Murdock and C. J. Horowitz, *ibid* C **35**, 1442 (1987); L. Ray and G. W. Hoffmann, *ibid.* **31**, 538 (1985); B. C. Clark, S. Hama, R. L. Mercer, L. Ray, G. W. Hoffmann, and B. D. Serot, *ibid.* C **28**, 1421 (1983).

[3]H. F. Arellano, F. A. Brieva, and W. G. Love, Phys. Rev. Lett. **63**, 605 (1989); Phys. Rev. C **41**, 2188 (1990).

[4]Ch. Elster, Taksu Cheon, Edward Redish, and P. C. Tandy, Phys. Rev. C **41**, 814 (1990).

[5]R. Crespo, R. C. Johnson, and J. A. Tostevin, Phys. Rev. C **41**, 2257 (1990).

[6]R. Machleidt, K. Holinde, and Ch. Elster, Phys. Rep. **149**, 1 (1987).

[7]M. Lacombe, B. Loiseau, J. M. Richard, R. Vinh Mau, J. Côté, P. Pirès, and R. de Tourreil, Phys. Rev. C **21**, 861 (1980).

[8]J. P. Dedonder and C. Schmit, Phys. Lett. **65**, B 131 (1976); J. P. Maillet, J. P. Dedonder, and C. Schmit, Nucl. Phys. **A271**, 253 (1976).

[9]A. L. Fetter and K. M. Watson, in *Advances in Theoretical Physics,* edited by K. A. Brueckner (Academic, New York,

1965), Vol. 1.
[10]A. K. Kerman, H. McManus, and R. M. Thaler, Ann. Phys. (N.Y.) **8**, 551 (1959).
[11]H. F. Arellano, F. A. Brieva, and W. G. Love, Phys. Rev. C **42**, 652 (1990).
[12]J. J. Kelly *et al.*, Phys. Rev. C **39**, 1222 (1989).
[13]E. J. Stephenson, J. Phys. Soc. Jpn. (suppl.) **55**, 316 (1985).
[14]D. A. Hutcheon *et al.*, Nucl. Phys. **A483**, 429 (1988); P. Schwandt, private communication.
[15]E. Bleszynski *et al.*, Phys. Rev. C **37**, 1527 (1988).